DOI : https://doi.org/10.56452/2023-04/004

ISSN: 0974-5823 Vol. 8 No. 4 April, 2023

International Journal of Mechanical Engineering

ANALYSIS OF SHELL AND HELICALLY COILED TUBE HEAT EXCHANGER PERFORMANCE WITH TIO2 NANOFLUID

Omar Ali Shabi [1], Majed Alhazmy[1], El-Sayed R. Negeed[1,2]

[1]*Faculty of Engineering, Department of Mechanical Engineering, Jeddah, King Abdulaziz University, P.O. Box 80204, Jeddah 21589, Saudi Arabia*

[2]*Reactors Department, Nuclear Research Center, Atomic Energy Authority, P.O. Box 13759 Cairo, Egypt*

ABSTRACT

The research aims to improve the heat transfer coefficient within the helical-coil pipe heat exchanger by combining water and titanium dioxide (TiO2) nanoparticles. In this work, the effects of nanofluids with different volumes Concentrations varying from.15 to.75 percent, the mass stream ratio of nanofluids inside the pipe, the mass stream ratios of water flow through the shell pipe, and the inlet temperature inside the tube on the Nusselt number were studied. Tests with and without nanoparticles were conducted under similar conditions. The test rig was constructed in the heat transfer laboratory, the it performed the tests and collected results. The test results show that nanoparticles enhance the heat transfer coefficient within the helically coiled tube significantly. The heat transfer coefficient inside the tube increases as the Reynolds number of the tube flow increases. Furthermore, the experimental findings reveal that when the Reynolds numbers increase, the friction factor of nanoparticle fluxes inside the tube decreases.

KEYWORDS: Heat exchanger, nanofluid, turbulent flow, heat transfer coefficient, pressure drop, Reynolds number, Friction Factor.

1. INTRODUCTION

The thermal performance and flow conditions of heat exchangers have significantly improved during the past few decades (Maghrabie et al., 2021; Huminic et al., 2016). The shell and helical coil heat exchanger is preferable to the typical shell and tube heat exchanger because it is small and can be utilised in high-temperature operations. As they provide a considerable fluid mix, shell and helical coil heat exchangers have a higher heat transfer coefficient than straight tube heat exchangers (Prabhanjan et al., 2002). In comparison to a straight tube, the flow of a working fluid in a coiled tube generates centrifugal force, leading to a secondary flow that improves heat transmission while increasing pressure drop. Cooling and conditioning systems, heat recovery activities, and food production all use shell and helically coil heat exchangers (Alimoradi and Veysi (2016) and Dravid (1971)). Traditional liquids, such as water and air, have low thermal conductivity, restricting thermal transfer rates. The thermal conductivity of standard heat transfer liquids can be increased by distributing nanoparticles across them without affecting their chemical or physical properties, resulting in a faster rate of heat transfer. Additionally, when nanoparticle volume fractions rise, so does the viscosity of the nanofluids, resulting in a higher pressure drop and, thus, higher energy inputs (Kumar and Chandrasekar (2020)). Many studies have been undertaken to investigate the thermo-physical properties of nanofluids to attain high heat conductivity while maintaining low viscosity (Fsadni et al. 2018). When dispersed and suspended uniformly in a fluid, a small number of nanoparticles improve the thermal properties of the base solution. Much research has demonstrated an increase in heat transfer due to the use of nanofluids within the helical coil tube for constant wall heat flux and constant wall heat (Kahani et al. (2013) and Tohidi et al. (2015)). Eiamsa-ard et al. (2018) studied the heat transmission of corrugated pipes with quasi-wing tapes experimentally. TiO2-water nanoparticles with three TiO2 concentrations (0.05 to 0.15 % by volume) were employed as working fluids, and semi-circular wing tapes with three wing angles (45 to 75 °) have been used as baffles in their examination. Reynolds employed tw-

wing configurations with numbers ranging from 8000 to 15,000. They discovered that corrugated pipes with semicircular wing tapes performed better in a parallel configuration than in acounterg configuration. Furthermore, when the wing angle grew, so did the heat transfer improvement. For instance, they reached the best thermal predictions for TiO2-water nanofluid at a concentration volume of 0.15 vol % at Reynolds number 8000, 1.98, by utilising coupled units in a parallel pattern at a wing angle of 75 °.

Maddah et al. (2014) investigated the heat transfer and total heat transfer of TiO2 nanofluids containing 0.01 vol percent in a twin-pipe heat exchanger. Nanofluids were combined with twisted-tape components in their research. The effects of temperature, mass flow rate, and nanoparticle concentration on the total heat transfer coefficient and variations in heat transfer were investigated in this study. Experiments were carried out in the turbulent flow regime and the counter-current flow regime. The coefficient of heat transmission increased by roughly 10 percent to 25 percent when nanofluids were combined with twisted tape. Srinivas and Vinod (2016) used three water-based nanomaterials to assess the efficiency of an agitated shell and helical coil heat exchanger (Al2O3, CuO, and TiO2). Various nano-fluid percentages, nanofluid temperatures, stir speeds, and coil-side fluid flow rates were used in the experiment. It was discovered that increasing the nanofluid concentration improved the heat transmission rate. Furthermore, heat exchanger efficacy was improved by increasing nanofluid concentration, stirring speed, and shell-side fluid temperature. Farajollahi et al. (2010) discovered that the heat transfer improvement of both nanoparticles is not the same at varied concentrations of nanoparticles. At low and high particle concentrations, TiO2-water and Al2O3-water nanomaterials perform better in terms of heat transmission. Conductivity and particle size competition between both nanomaterials could be the source of these disparities in thermophysical properties. From the above literature review, while previous studies have explored the heat transfer features of a nanofluid stream inside the shell and helical coil tube heat exchanger both experimentally and computationally, there is no published numerical analysis of a nanofluid stream through the shell and helical coil tube heat exchanger that considers conjugate heat transfer amongst the hot and cold liquids. This thesis presented the heat transfer and performed analysis of TiO2/water nanofluids in a shell and helically coiled tube heat exchanger considering fluid-fluid heat transfer.

2. EXPERIMENTAL WORK

Figure 1 below illustrates the experimental setup's schematic chart. Before beginning the experiments, the cold and hot water tanks are filled, and the required amount of nanoparticles are weighed. The weighted nanoparticles are then added and mixed inside the hot water tank with thorough mixing. After that, start the heaters inside the hot water tanks to heat up the solution in the tank with the help of a fire stove until the solution reaches the required temperature. The tests begin once the mixture temperature within the hot tank reaches the needed temperature, while the cold-water temperature remains constant during all tests (30 oC). The first step in forming the test is opening the water valves for the inlet pips in the tube and shell and adjusting the water flow speeds using the flowmeter. In contrast with opening the water valves, the cold and hot pumps are turned on. Pumps will pressurise the water in the tube and shell, the nanofluid will flow through the inner tube, and the cold water will flow through the annulus of the helically coiled heat exchanger. The Omega program also starts recording the experimentation temperature at every spot linked to the thermocouples. The test takes around 20 to 25 minutes. Once the time is up, the pumps turn off, and shell and tube valves shut off. Also, the collected data from the Omega program is saved. With the last step completed, the experiment will be finished. For the next test run with a different amount of nanofluids, the nanofluids tank is reheated to the required temperature, the temperature of the cold water and nanofluids tank is measured, and the flowmeters are adjusted according to the required flow rates. The same procedures are then repeated for all the nanoparticles required.

DOI : https://doi.org/10.56452/2023-04/004

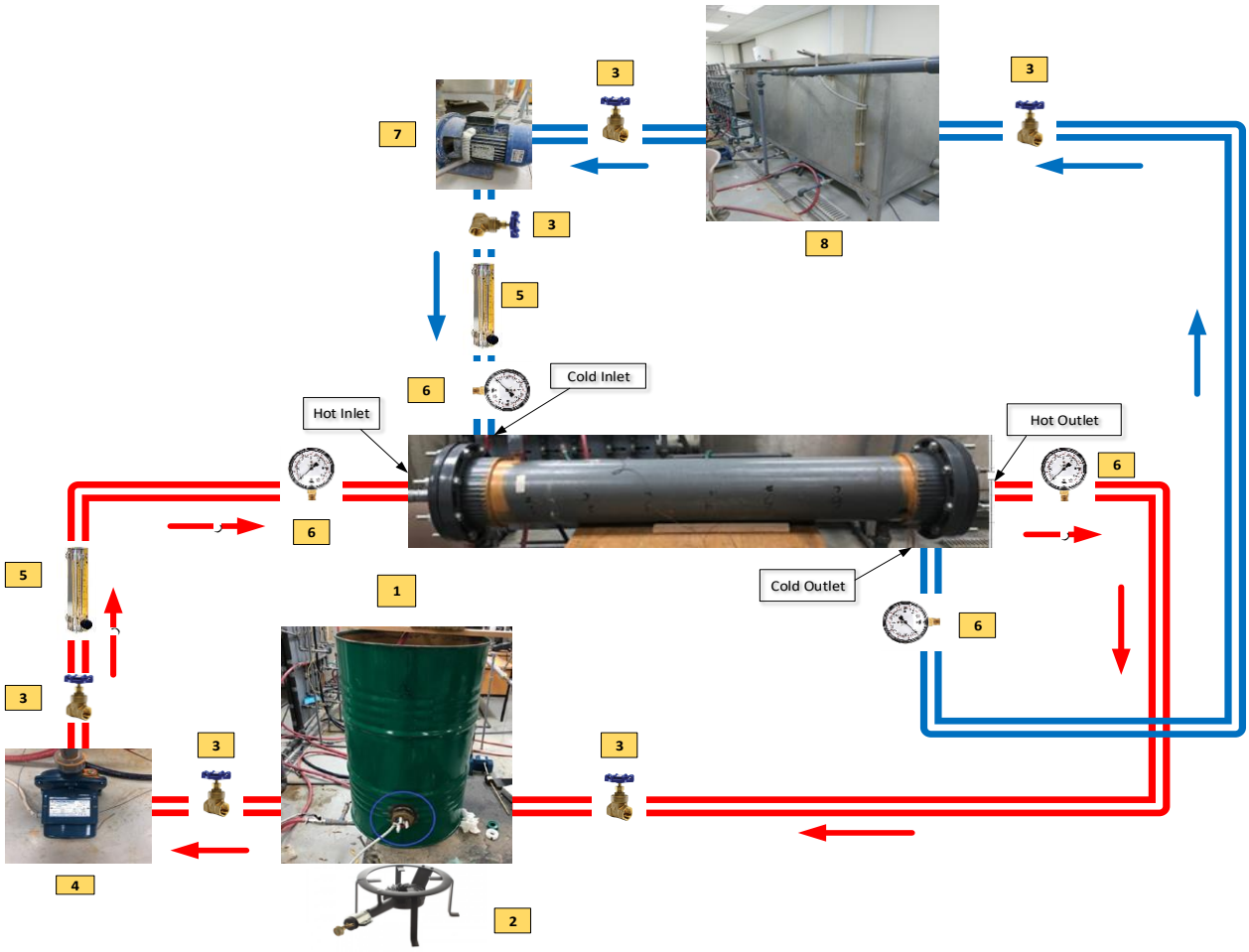

1	Hot water tank	5	Flowmeter
2	Propane stove	6	Pressure gage
3	Ball valve	7	Cold water pump
4	Hot water pump	8	Cold water tank.

Figure 1 Schematic diagram for experiment setup

3. METHODOLOGY

Determination of the thermophysical properties of nanofluid:

The volume concentration of nanofluid can be determined as:

$$\text{Volume concentration (\%)}, \Phi = \left[\frac{\left(\frac{W_{Al_2O_3}}{\rho_{Al_2O_3}}\right)}{\left(\frac{W_{Al_2O_3}}{\rho_{Al_2O_3}}\right)\left(\frac{V_{water}}{\rho_{water}}\right)}\right] \quad (1)$$

The viscosity of nanofluid can be determined as:

$$\mu_{nf} = \mu_{bf}(1 + 2.5\phi) \quad (2)$$

The density of nanofluid can be determined as:

$$\rho_{nf} = \phi\rho_p(1-\phi)\,\rho_{bf} \quad (3)$$

The specific heat at constant pressure of nanofluid can be determined as:

$$C_{p,nf} = \phi C_p(1-\phi)\,C_{bf} \quad (4)$$

The solid-liquid mixture thermal conductivity can be defined by Maxwell (1904) as:

$$k_{nf} = k_{bf}\left[\frac{k_p+2k_{bf}+2\emptyset(k_p-k_{bf})}{k_p+2k_{bf}-\emptyset(k_p-k_{bf})}\right] \quad (5)$$

The heat transfer rate of the annulus can be determined as:

$$Q_c = \dot{m}_c\, C_{p,c}\left(T_{c,out} - T_{c,in}\right) \quad (6)$$

The heat transfer rate of the nanofluid can be determined as:

$$Q_{nf} = \dot{m}_{nf}\, C_{p,nf}\left(T_{nf,in} - T_{nf,out}\right) \quad (7)$$

The heat transfer rate average can be determined as:

$$Q_{avg} = \left(Q_{nf} + Q_c\right)/2 \quad (8)$$

The overall heat transfer coefficient without considering the fouling factor term can be determined as:

$$U_{in} = \frac{Q_{avg}}{A_{in}\,\Delta T_{lm}},\ \Delta T_{lm} = \frac{\left(T_{nf,in}-T_{c,in}\right)-\left(T_{nf,out}-T_{c,out}\right)}{ln\left(\frac{T_{nf,in}-T_{c,in}}{T_{nf,out}-T_{c,out}}\right)} \quad (9)$$

Where: $A_{in} = \pi d_{in} L$, L= length of helical coil

The heat transfer coefficient of the outer tube flow evaluated by the equation:

$$h_{out} = \frac{Nu_{out}K_{out}}{d_{eqv}} \quad (10)$$

Here d_{eqv} will be estimated by:

$$d_{eqy} = \left(D_i^2 \_ d_o^2\right)/d_o \quad (11)$$

The heat transfer coefficient of the nanofluid without considering fouling can be found using the following formula:

$$\frac{1}{U_{in}A_{in}} = \frac{1}{h_{in}A_{in}} + \frac{ln\left(\frac{d_o}{d_i}\right)}{2\pi kl} + \frac{1}{h_{out}A_{out}} \quad (12)$$

Where: $d_i = inner\ diameter\ of\ the\ helical\ coil$

$d_o = outer\ diameter\ of\ the\ helical\ coil$

k = thermal conductivity

The Reynolds number in the internal tube, the formula is given:

$$\text{Re} = \frac{4\dot{m}_{nf}}{\pi d_i\, \mu_{nf,i}} \quad (13)$$

The Nusselt number of mono/hybrids nanofluid will be considered using:

$$Nu_{nf} = h_{nf} d_i / k_{nf} \quad (14)$$

The Number of transfer units (NTU) of the nanofluid can be determined as:

$$\text{NTU} = \frac{UA}{C_{min}} \quad (15)$$

Where: $C_h = m_h \dot{C}_{p_h}$, $C_c = m_c \dot{C}_{p_c}$, C_{min} is the minimum value of $C_h\ and\ C_c$.

The heat exchanger effectiveness (ϵ) can be determined as:

$$\varepsilon = \frac{Q_{actual}}{Q_{max}} \quad (16)$$

Where: $Q_{max} = C_{min}\dot{\Delta}T_{max}$, $\Delta T_{max} = T_{h,i} - T_{c,i}$

Or:

DOI : https://doi.org/10.56452/2023-04/004

$$\varepsilon = \frac{1-\exp[-NTU(1-Cr)]}{1-\mathrm{Cr}\exp[-NTU(1-Cr)]} \quad (17)$$

Where: $C_r = \frac{C_{min}}{C_{max}}$

The fraction factor (F) of the nanofluid can be determined as:

$$F = \frac{\Delta P}{\frac{L}{di}(\frac{\rho_{nf} u_{nf}^2}{2})} \quad (18)$$

Where: $\Delta P = P_{in} - P_{out}$

4. RESULTS AND DISCUSSIONS

4.1 Effects of Reynolds number and nanofluid on Nusselt number

Figure 2 demonstrates the impact of the Reynolds number and varied volume concentrations of nanofluid on the Nusselt number at a mass flow rate of 0.166 kg/s and temperatures of (a) 65 °C, (b) 70 °C, and (c) 75 °C, correspondingly. The figure shows that the pattern of the Nusselt number (Nu), which is based on the inner diameter of the tube, is the same for the nanofluid and pure water under identical conditions. However, the nanofluid yielded a substantially higher Nu. The Nusselt number tends to grow considerably when the volume concentration ratio for TiO2 nanofluid increases from 0% to 0.30%, and the Nusselt number reaches its ideal value at 0.30% volume concentration of nanoparticles. This is a result of the tube's decreased temperature difference, decreased specific heat at constant pressure, and increased thermal conductivity. Additionally, as concentrations increase above 0.30 percent, the Nusselt number is slightly impacted because the nanoparticles gather in fouling layers inside the tube, which inhibits heat transfer. The Nu increases as the Reynolds number of the flow inside the tube increases. That is a result of the impact of increased turbulent flow. The present findings are consistent with those of Niwalkar et al. (2019), Shahrul et al. (2016), Suresh et al. (2011), Naik and Vinod (2018), and Ardekani et al. (2019), who discovered that a higher Reynolds number can increase convective heat transfer. Additionally, the Nu increases as the flow temperature of the nanofluids increases. This result is due to a decrease in the viscous force brought on by an increase in the bulk temperature, which leads to an increase in convective heat transfer. This result is in line with those of related studies by Niwalkar et al. (2019), Shahrul et al. (2016), and Ardekani et al. (2019), which show that, under the same conditions, the convective heat transfer increases as the inlet bulk temperature increases.

DOI : https://doi.org/10.56452/2023-04/004

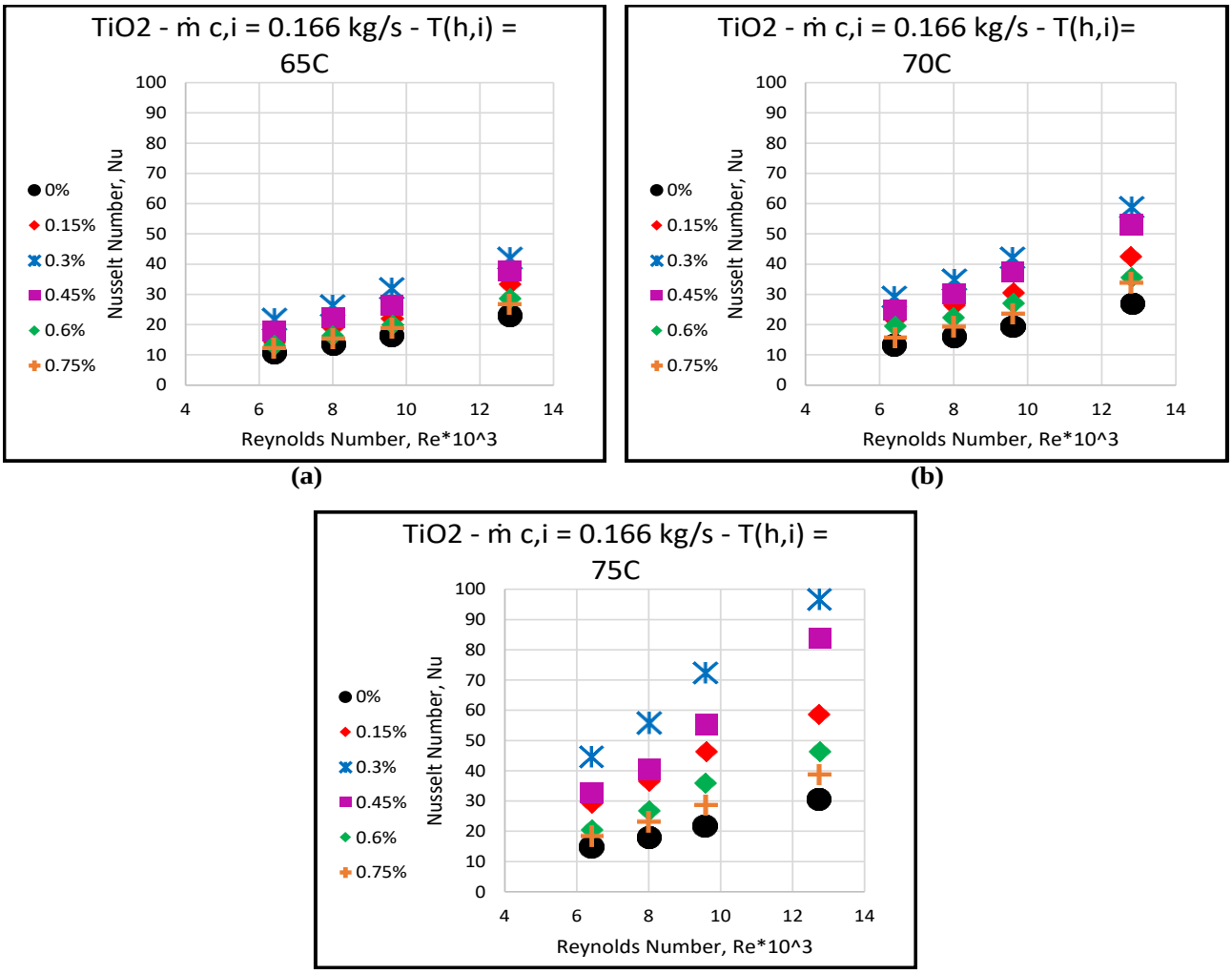

Figure 2 Effects of the Reynolds number on the Nusselt number of water and TiO_2 nanofluid at different particle concentrations, at the mass flow rate of the shell, is 0.166 kg/s, and at different temperatures of (a) 65°C, (b) 70°C, and (c) 75°C

At a mass flow rate of 0.2 kg/s and temperatures of (a) 65°C, (b) 70°C, and (c) 75°C, respectively, the effects of Reynolds number and nanofluid with varying volume concentrations on the Nusselt number are shown in Figure (3). As the temperature of the inflow nanofluid in the tube increases, the Nusselt number increases as well.

DOI : https://doi.org/10.56452/2023-04/004

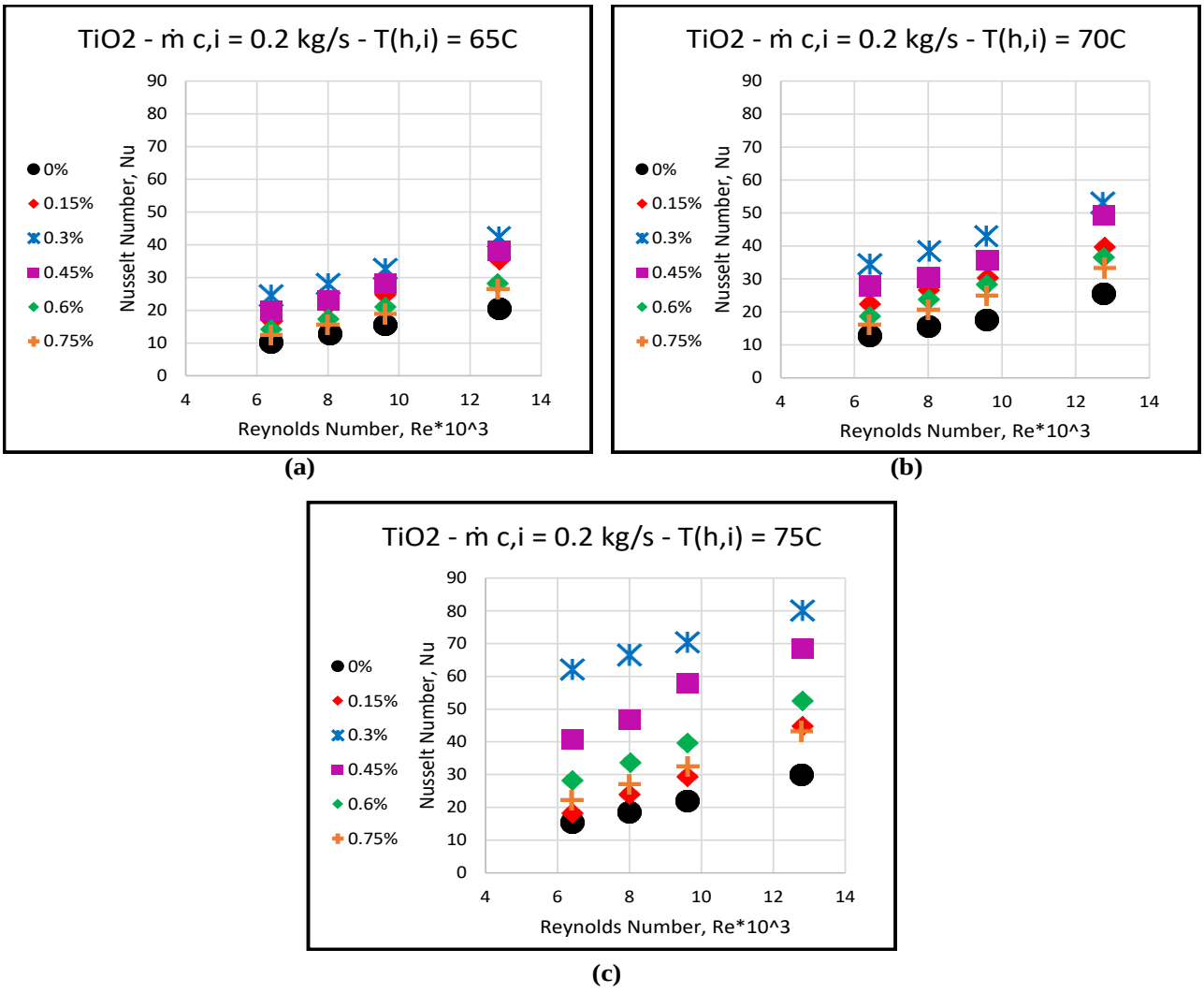

Figure 3 Effects of the Reynolds number on the Nusselt number of water and TiO_2 nanofluid at different particle concentrations, at a mass flow rate of the annulus, is 0.2 kg/s, and at different temperatures of (a) 65°C, (b) 70°C, and (c) 75°C

Figure (4) shows the impact of the Reynolds number and nanofluid with varied volume concentrations on the Nusselt number when the annulus mass flow rate is 0.25 kg/s and the temperatures are (a) 65°C, (b) 70°C, and (c) 75°C, respectively. The Nusselt number was found to grow when the inflow nanofluid temperature in the tube increased. Additionally, the Nu increases as the temperature of the nanofluids flow increases. This outcome is the result of a reduction in viscous force brought about by an increase in bulk temperature, which causes an increase in convective heat transfer, as mentioned before.

DOI : https://doi.org/10.56452/2023-04/004

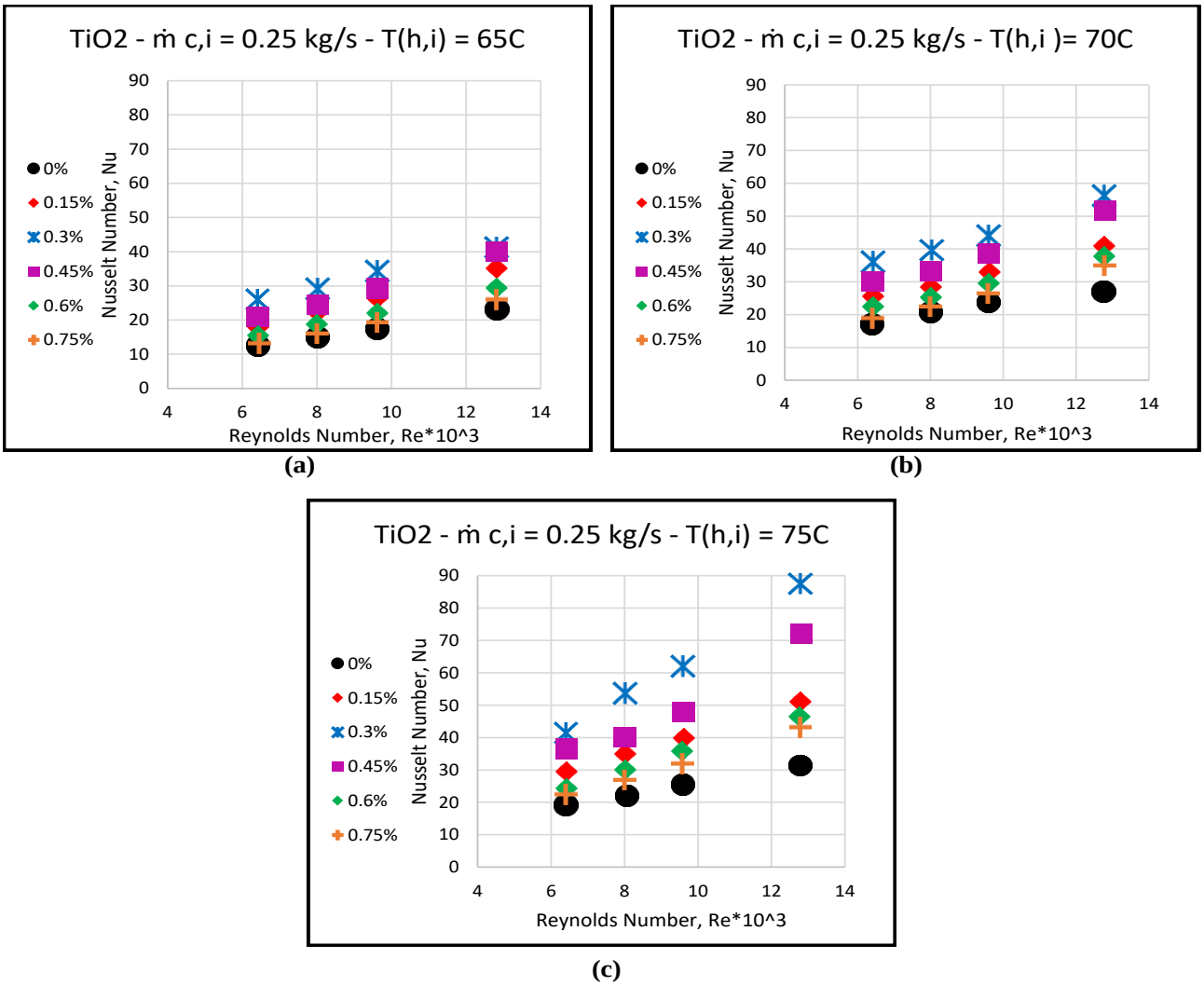

Figure 4 Effects of the Reynolds number on the Nusselt number of water and TiO_2 nanofluid at different particle concentrations, at the mass flow rate of the annulus, which is 0.25 kg/s, and at different temperatures of (a) 65°C, (b) 70°C, and (c) 75°C

Figures 3, 4, and 2 shown that the Nusselt number increases as the mass flow rate the nanofluids through the inner tube increases. That is because of an increase in the turbulent flow. Also, the nanoparticle has a substantial influence on increasing the Nusselt number, and the volume concentration at which the Nusselt number is at its highest is 0.30 percent.

4.2 Effects of Reynolds number and nanofluid on the Number of transfer units

Figure (5) shows the influence of the Reynolds number and different volume concentrations of nanofluid on the number of transfer units at a mass flow rate of 0.166 kg/s and temperatures of (a) 65 °C, (b) 70 °C, and (c) 75 °C, respectively. As shown in the figures, the number of transfer units decreases with an increase in the Reynolds number, as the Reynolds number increases with the mass flow rate, yet the number of transfer units has an inverse relationship with the mass flow rate. This is because the minimum specific capacity (Cmin) increases as the mass flow rate of the nanofluid inside the tube increases, and it is known that the NTU is inversely proportional to the Cmin. Also, the nanofluids have significant developments in the number of transfer units as it increases with increased volume concentrations of particles, which is due to the increase in thermal conductivity and surface area. Additionally, the nanofluids have a considerable enhancement in the number of transfer units as the volume concentration increases from 0% to 0.30 %. increasing the volume concentration above this amount leads toa reduction in the number of transfer units, which is related to the impacts of increasing the specific heat at constant pressure and mass flow rate. Furthermore, the highest enhancement of the number of transfer units for nanofluid is particularly significant at their optimum with nanoparticle volume concentrations of 0.30%. The NTU increases as the

DOI : https://doi.org/10.56452/2023-04/004

inlet temperature of the nanofluid increased, which is due to the increase in the heat transfer coefficient inside the tube (hi)as well as the increase in the bulk temperature as mentioned previously.

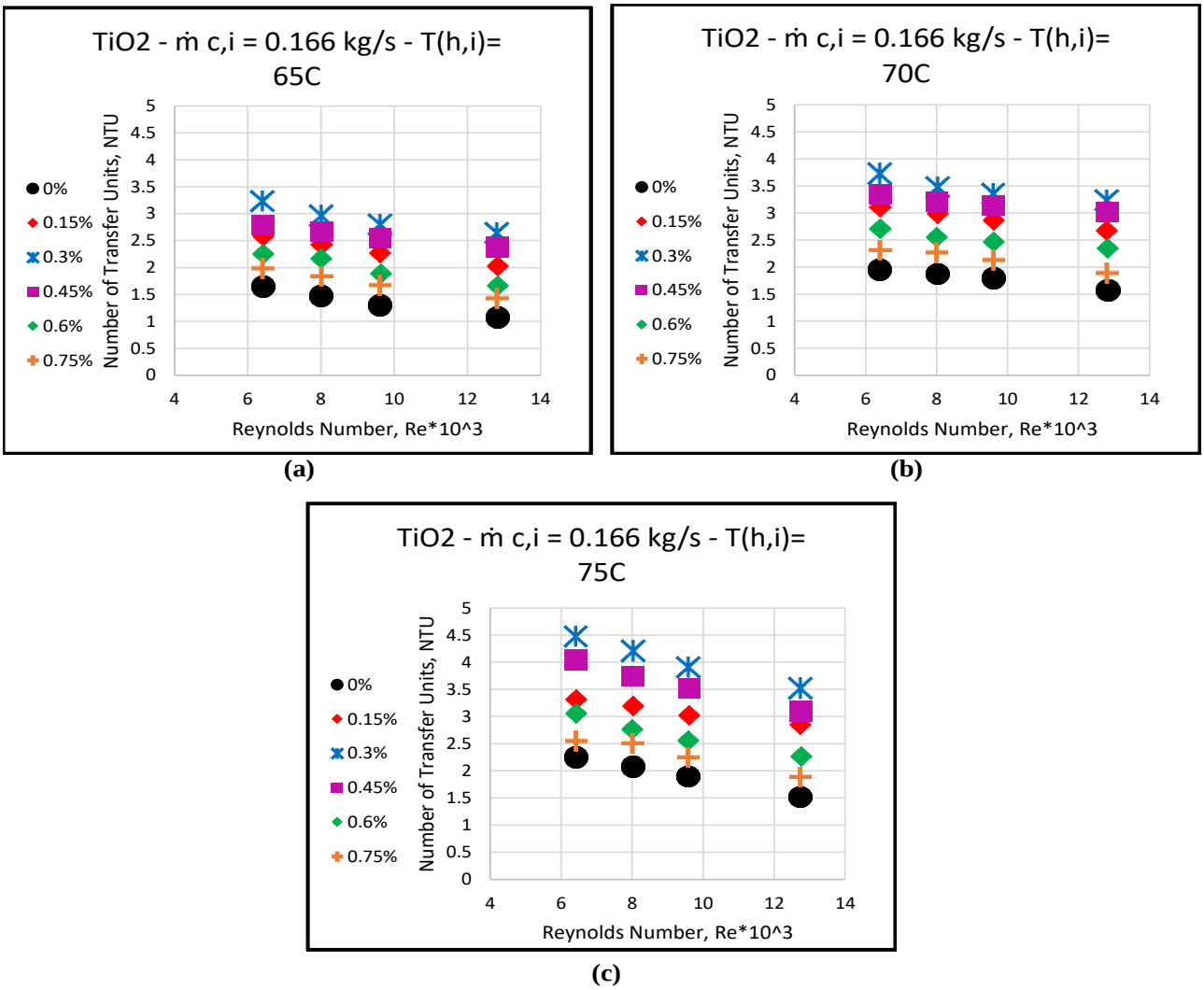

Figure 5 Effects of the Reynolds number on the NTU of water and TiO_2 nanofluid at different particle concentrations, at the mass flow rate of the annulus, is 0.166 kg/s, and at different temperatures of (a) 65°C, (b) 70°C, and (c) 75°C

Figure (6) shows the effects of the Reynolds number and nanofluid with different volume concentrations on the Number of transfer units, at the mass flow rate of the annulus is 0.2 kg/s and at different temperatures of (a) 65°C, (b) 70°C, and (c) 75°C respectively.

DOI : https://doi.org/10.56452/2023-04/004

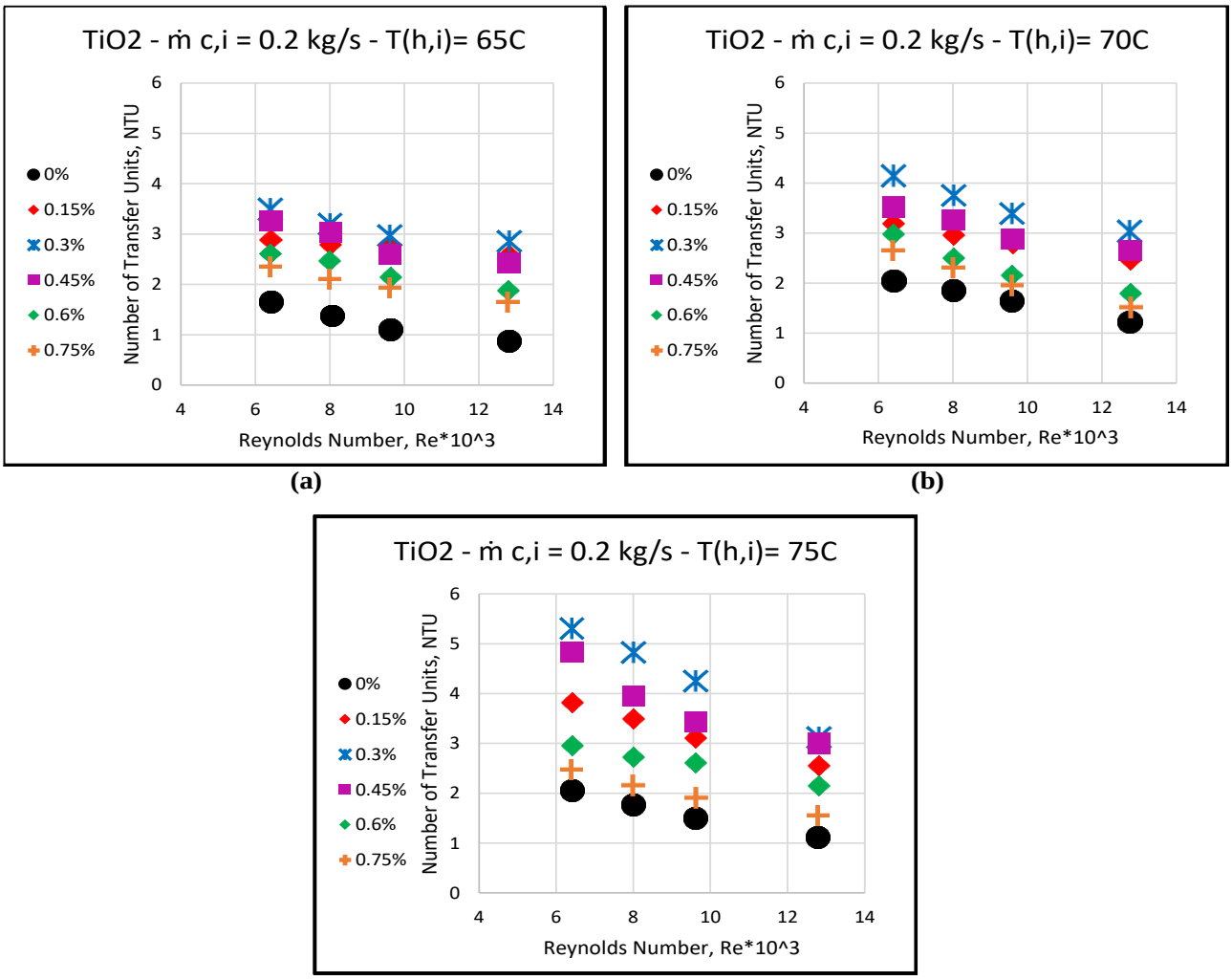

Figure 6 Effects of the Reynolds number on the NTU of water and TiO_2 nanofluid at different particle concentrations, at a mass flow rate of the annulus, is 0.2 kg/s, and at different temperatures of (a) 65°C, (b) 70°C, and (c) 75°C

Figure (7) shows the effects of the Reynolds number and nanofluid with different volume concentrations on the Number of transfer units, at the mass flow rate of the annulus is 0.25 kg/s and at different temperatures of (a) 65°C, (b) 70°C, and (c) 75°C respectively

DOI : https://doi.org/10.56452/2023-04/004

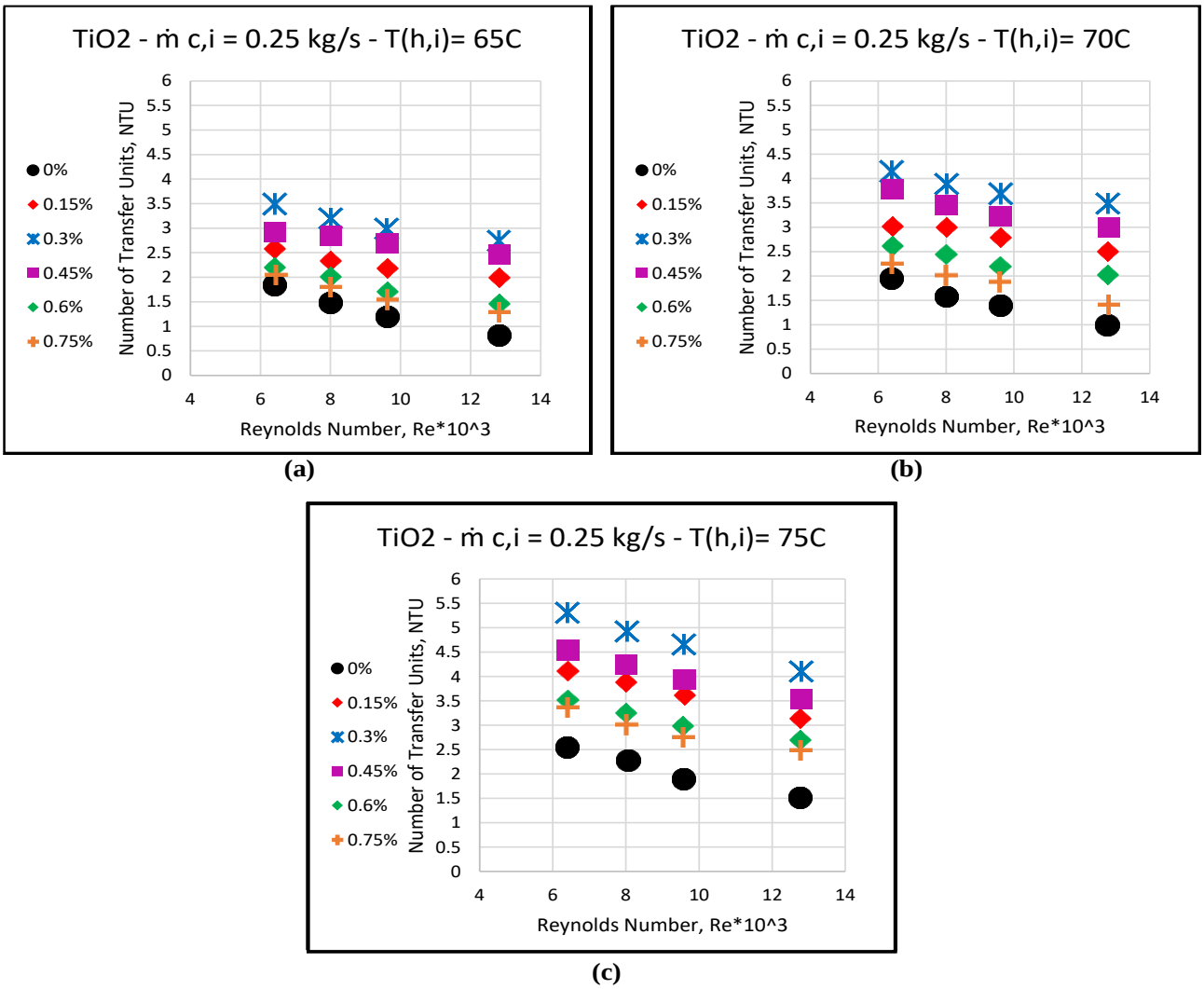

Figure 7 Effects of the Reynolds number on the NTU of water and TiO_2 nanofluid at different particle concentrations, at the mass flow rate of the annulus, which is 0.25 kg/s, and at different temperatures of (a)65°C, (b) 70°C, and (c) 75°C

Figures 6 and 7 show identical behaviour to that in Figure 5, whereas the Reynolds number increases and the number of transfer units decreases. The nanoparticle has a significant effect on the increase in the number of transfer units, and the value of the volume concentration at which the number of transfer units is at its maximum is 0.30%. From figures 5–7, it was shown that the NTU decreases as the mass flow rate of the inner tube increases. This is because the minimum specific capacity (C_{min}) increases as the mass flow rate of the nanofluid inside the tube increases, and it is known that the NTU is inversely proportional to the C_{min}.

4.3 Effects of Reynolds number and nanofluid on Effectiveness

At a mass flow rate of 0.166 kg/s and various temperatures of approximately: (a) 65°C, (b) 70°C, and (c) 75°C, respectively. Figure 8 depicts the impact of the Reynolds number and nanofluid with varied volume concentrations on the effectiveness. As well, effectiveness declines because of the transition from laminar to turbulent flow. Additionally, the effectiveness value increases as the volume concentration of nanofluid grows since a higher concentration of nanoparticles in the fluid will enhance its conductivity, which in turn will speed up heat transfer and ultimately increase effectiveness. This finding is consistent with findings from earlier research by Shahrul et al. (2016): The ultimate value of effectiveness occurs when the volume concentration of the nanoparticles is around 0.30%. After this value, increasing the volume concentration has a negligible impact on the effectiveness because the nanoparticles accumulate and create fouling layers that avoid heat transfer.

DOI : https://doi.org/10.56452/2023-04/004

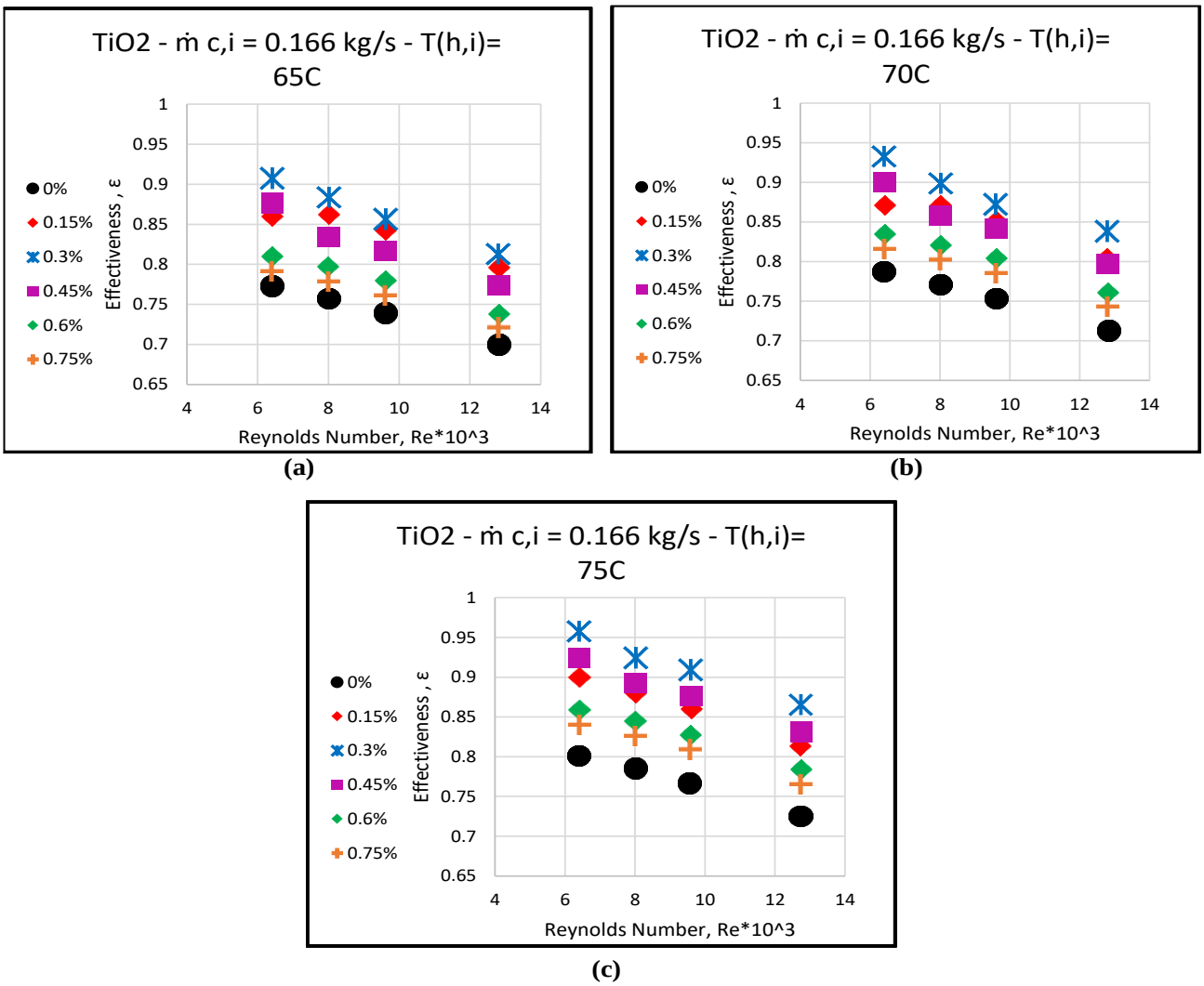

Figure 8 Effects of the Reynolds number on the Effectiveness of water and TiO_2 nanofluid at different particle concentrations, at the mass flow rate of the annulus, is 0.166 kg/s, and at different temperatures of (a)65°C, (b) 70°C, and (c) 75°C

Figure (9) shows the effects of the Reynolds number and nanofluid with different volume concentrations on the Effectiveness, at the mass flow rate of the annulus is 0.2 kg/s and at different temperatures of about: (a) 65°C, (b) 70°C, and (c) 75°C respectively.

DOI : https://doi.org/10.56452/2023-04/004

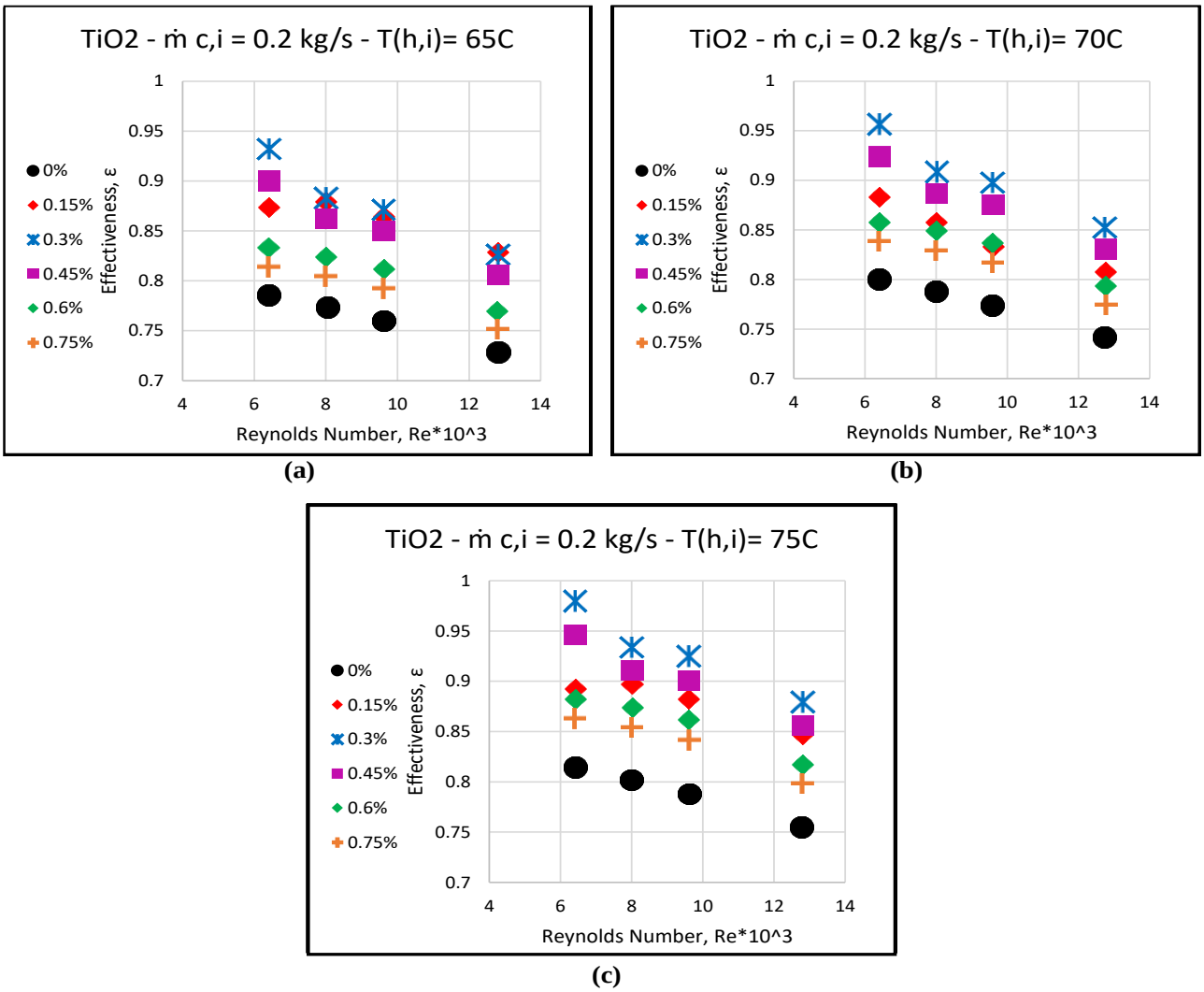

Figure 9 Effects of the Reynolds number on the Effectiveness of water and TiO_2 nanofluid at different particle concentrations, at the mass flow rate of the annulus, which is 0.2 kg/s, and at different temperatures of (a) 65°C, (b) 70°C, and (c) 75°C

Figure (10) shows the effects of the Reynolds number and nanofluid with different volume concentrations on the Effectiveness, at the mass flow rate of the annulus is 0.25 kg/s and at different temperatures of about: (a) 65°C, (b) 70°C, and (c) 75°C respectively.

DOI : https://doi.org/10.56452/2023-04/004

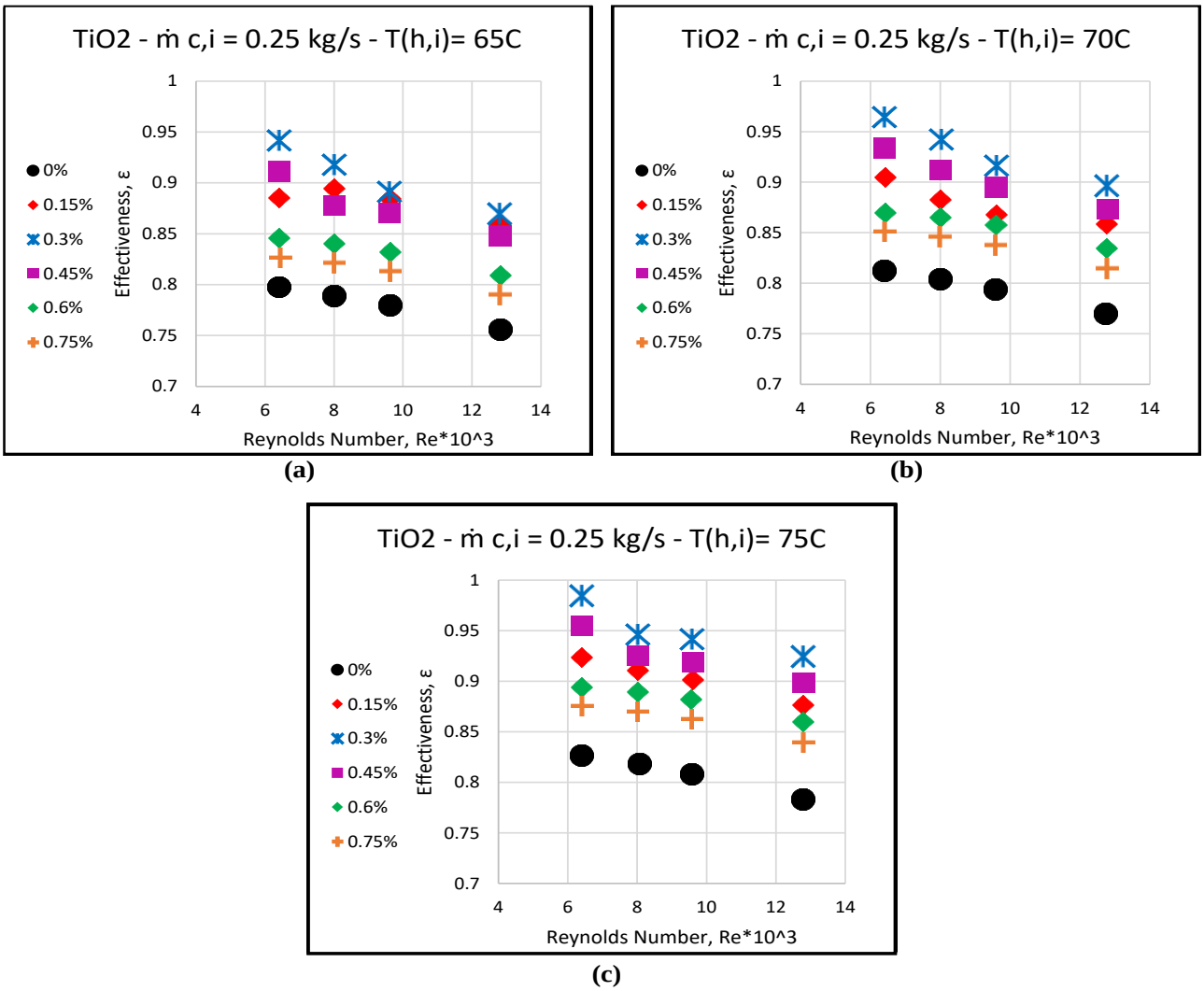

Figure 10 Effects of the Reynolds number on the Effectiveness of water and TiO_2 nanofluid at different particle concentrations, at the mass flow rate of the annulus, which is 0.25 kg/s, and at different temperatures of (a) 65°C, (b) 70°C, and (c) 75°C

The above Figures 8, 9, and 10 show identical behavior, whereas as the Reynolds number increases, the effectiveness decreases. The nanoparticle has an influential effect on increasing the effectiveness, and the value of the volume concentration at which the effectiveness is at its highest is 0.30%. From figures 8–10, it was shown that the effectiveness decreases as the mass flow rate of the inner tube increases. This is because the maximum heat transfer increases as the mass flow rate of the nanofluid inside the tube increases.

4.4 Effects of Reynolds number and nanofluid on friction factor

Figure (11) shows the impacts of the Reynolds number and nanofluid with different volume concentrations on the friction factor, at the mass flow rate of the annulus is 0.166 kg/s and at different temperatures of (a) 65°C, (b) 70°C, and (c) 75°C respectively. As illustrated in the figures, as the Reynolds number inside the tube increases, the friction factor decreases. This is because increasing the Reynolds number will create a turbulent flow, which causes a decrease in the friction coefficient. Furthermore, increasing the particle volume concentrations results in an increase in the friction factor, and this increase is due to an increase in the density and the viscosity of the nanofluid, which leads to more pressure drops. This result is in line with the results from relevant work by Niwalkar et al. (2019), K. Singh et al. (2021), and Kumar et al. (2013), where they found that increasing Reynolds number causes a decrease in friction factors. The nanofluids have a substantial effect on the friction factor, where increasing the volume concentration significantly increases the friction factor. The regression friction coefficient somewhat decreases as the inlet temperature of the nanofluid to the tube increases. That is due to the decrease in viscosity with the increase in the inlet bulk temperature.

DOI : https://doi.org/10.56452/2023-04/004

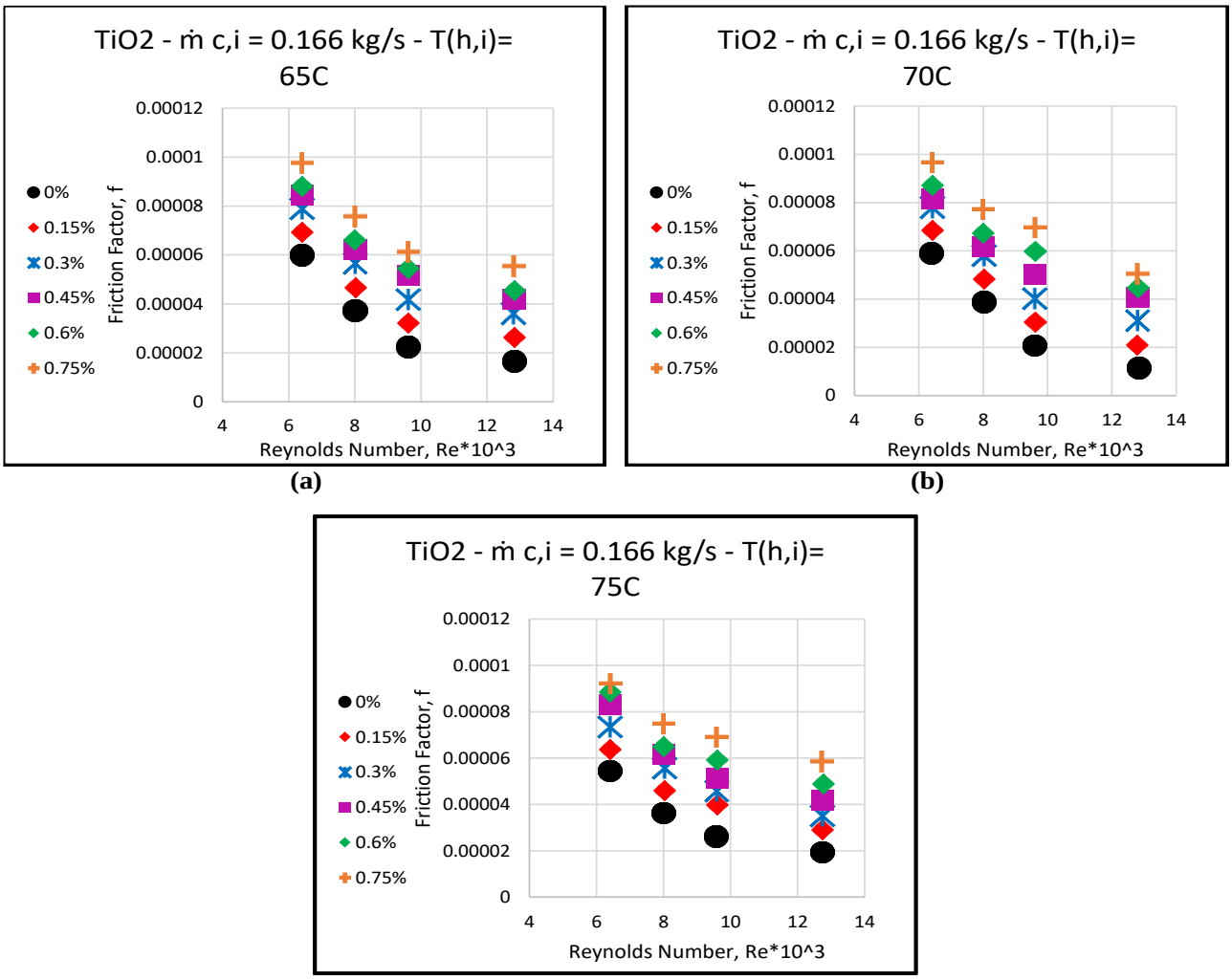

Figure 11 Effects of the Reynolds number on the fraction factor of water and TiO_2 nanofluid at different particle concentrations, at the mass flow rate of the annulus, is 0.166 kg/s, and at different temperatures of (a) 65°C, (b) 70°C, and (c) 75°C

Figure (12) shows the effects of the Reynolds number and nanofluid with different volume concentrations on the friction factor, at the mass flow rate of the annulus is 0.2 kg/s and at different temperatures of about: (a) 65°C, (b) 70°C, and (c) 75°C respectively.

DOI : https://doi.org/10.56452/2023-04/004

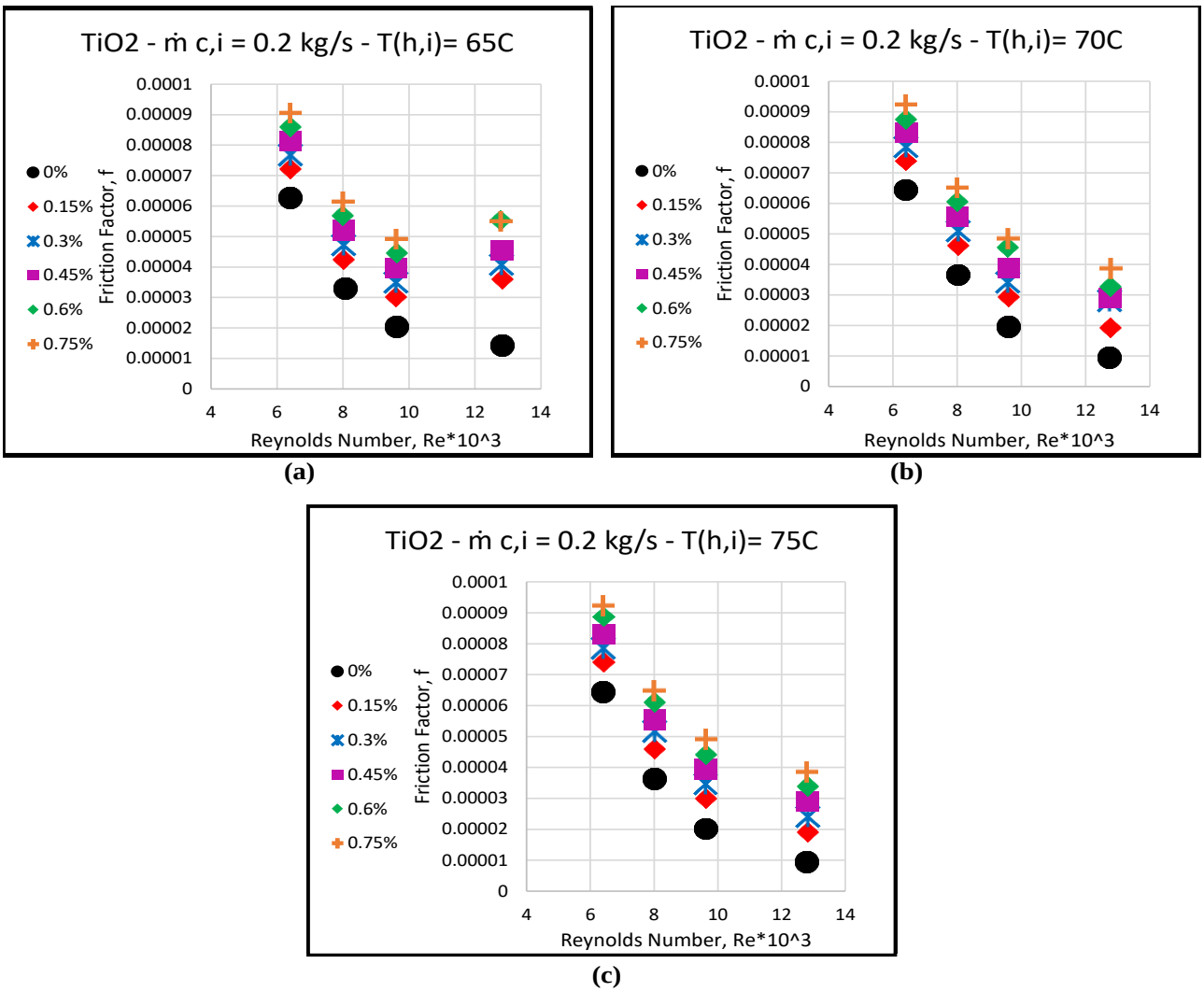

Figure 12 Effects of the Reynolds number on the fraction factor of water and TiO_2 nanofluid at different particle concentrations, at the mass flow rate of the annulus, is 0.2 kg/s, and at different temperatures of (a) 65°C, (b) 70°C, and (c) 75°C

Figure (13) shows the effects of the Reynolds number and nanofluid with different volume concentrations on the friction factor, at the mass flow rate of the annulus is 0.25 kg/s and at different temperatures of about: (a) 65°C, (b) 70°C, and (c) 75°C respectively.

DOI : https://doi.org/10.56452/2023-04/004

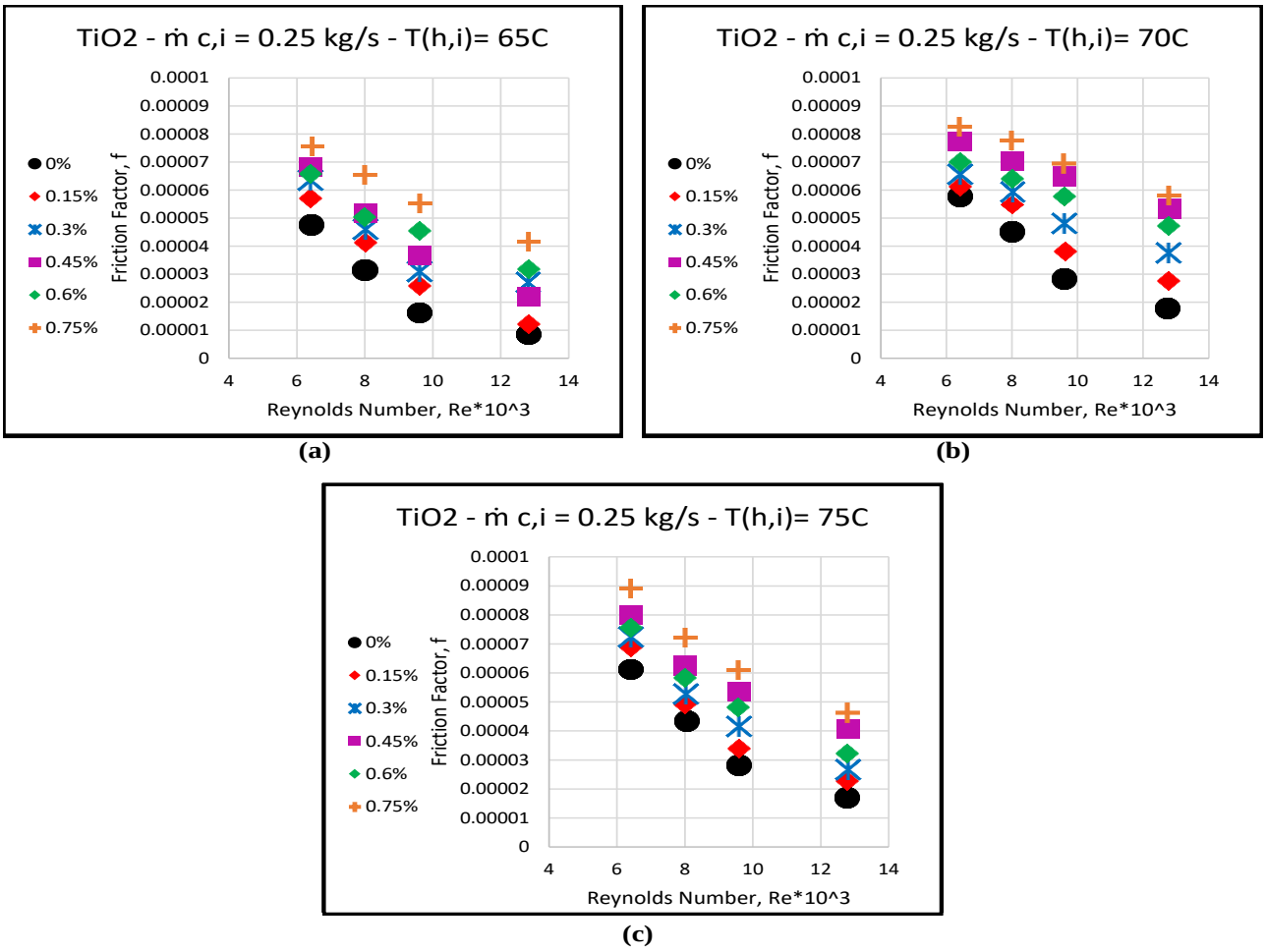

Figure 13 Effects of the Reynolds number on the fraction factor of water and TiO_2 nanofluid at different particle concentrations, at the mass flow rate of the annulus, is 0.25 kg/s, and at different temperatures of (a) 65°C, (b) 70°C, and (c) 75°C

Figures 11, 12, and 13 display similar behavior, as the Reynolds number increases, the fraction factor decreases. The nanoparticle has a marked effect on the increase of the fraction factor and the value of the volume concentration at which the fraction factor is the highest value is 0.75%. From the figures 11-13, it is observed that the regression friction coefficient decreases as the mass flow of the nanofluid to the tube increases. That is due to the increase in the inertia force with the increase in the inlet mass flow rate.

4.5 Empirical Equations

Empirical correlations can be derived from the experimental data to reflect the relationships for the parameters impacting the Nusselt number and fraction factor. These parameters are the Reynolds number in the helical coil, the Reynolds number in the shell, the Prandtl number, and the volume concentration of the nanofluid. Table (1) below lists the ranges of these parameters for TiO_2 nanoparticles:

Table 1. Parameters range for TiO_2 nanoparticle

TiO_2	Re (nf)	Re (bf)	Pr	Volume concentration	The temperature in the coil	The temperature in the annulus	Pressure drops in the coil
Max value	12829.24	13683.14	5.1248	0.75%	52℃	32.5 ℃	19 kPa
Min value	6387.26	8661.45	4.4378	0.0%	22℃	22.1 ℃	8 kPa

DOI : https://doi.org/10.56452/2023-04/004

- The results of the experiments have shown that the correlation between the Nusselt number and the friction factor can be established within tolerance values of ±20%.

4.5.1 TiO_2 with volume concentration of 0.0% to 0.30%

The empirical relation for the Nusselt number is found to be:

$$Nu_{nf} = 6.808 \times 10^{-7} \times {Re_{nf}}^{0.9} \times {Re_{bf}}^{3.43} \times Pr^{0.388} \times (1+\phi)^{277.098}$$

The comparison between the predicted Nusselt number value of the above equation and the experimental value for the volume concentration ranges $0\ \% \leq \phi \leq 0.30\%$ is shown in Figure 14. It is shown that prediction results agree with the experimental data very well with deviation of ±15%.

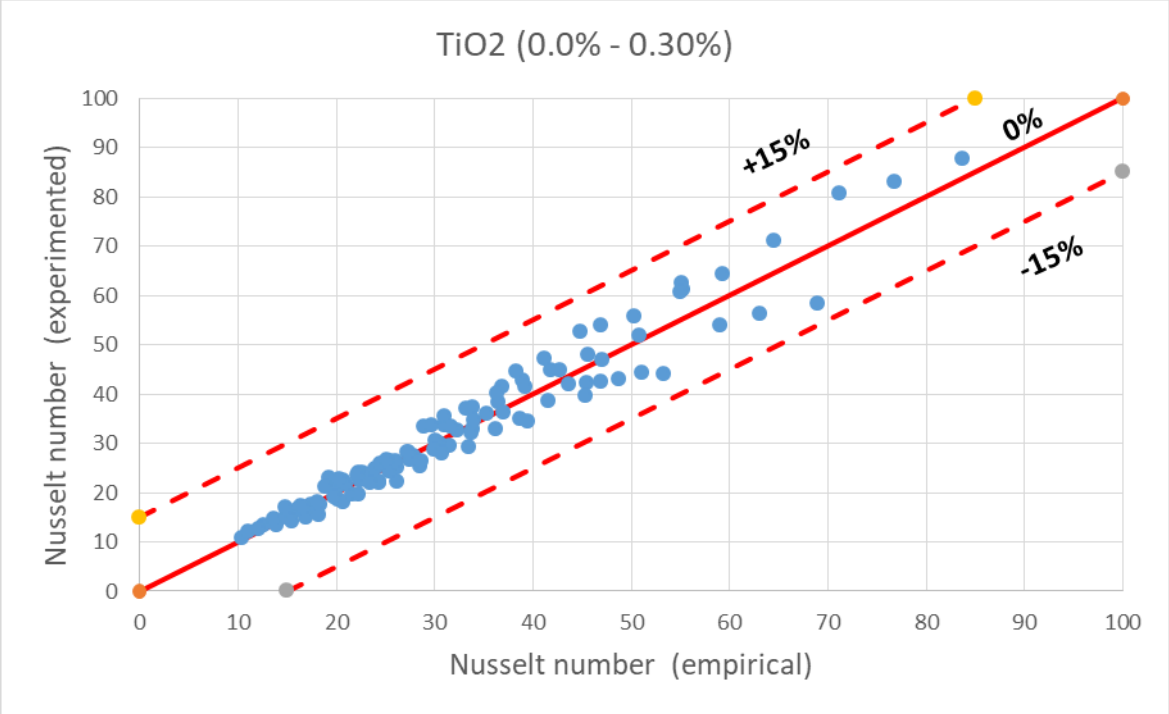

Figure 14 Relationship between the experimental and empirical results of $\mathbf{Nu_{nf}}$ maximum for TiO_2 nanofluid

4.5.2 TiO_2 with volume concentration of 0.30% to 0.75%

The empirical relation for the Nusselt number is found to be:

$$Nu_{nf} = 4.435 \times 10^{-6} \times {Re_{nf}}^{0.922} \times {Re_{bf}}^{3.971} \times Pr^{0.21} \times (1+\phi)^{-149.191}$$

The relationship between the predicted Nusselt number value of the above equation and the experimental value for the volume concentration ranges $0.30\ \% \leq \phi \leq 0.75\%$ is displayed in Figure 15. It is demonstrated that prediction results agree with the experimental data very well with deviation of ±15%.

DOI : https://doi.org/10.56452/2023-04/004

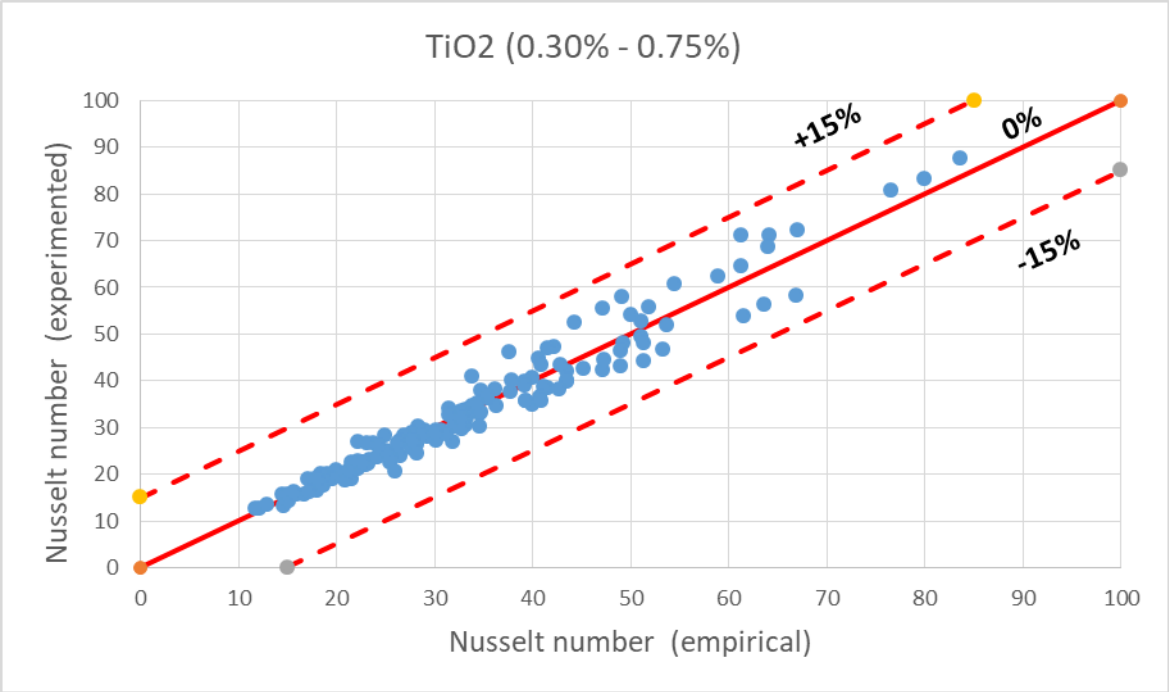

Figure 15 Relationship between the experimental and empirical results of Nu_{nf} minimum for TiO_2 nanofluid

4.5.3 TiO_2 with volume concentration of 0.0% to 0.75%

The empirical relation for the Friction factor is found to be:

$$F_{reg} = 3.912 \times Re_{nf}^{-1.287} \times (1+\phi)^{100.597}$$

The comparison between the predicted fraction factor value of the previous equation and the experimental value for the volume concentration ranges $0\ \% \leq \phi \leq 0.75\%$ is shown in Figure 16. It is shown that prediction results agree with the experimental data very well with the maximum deviation ±20%.

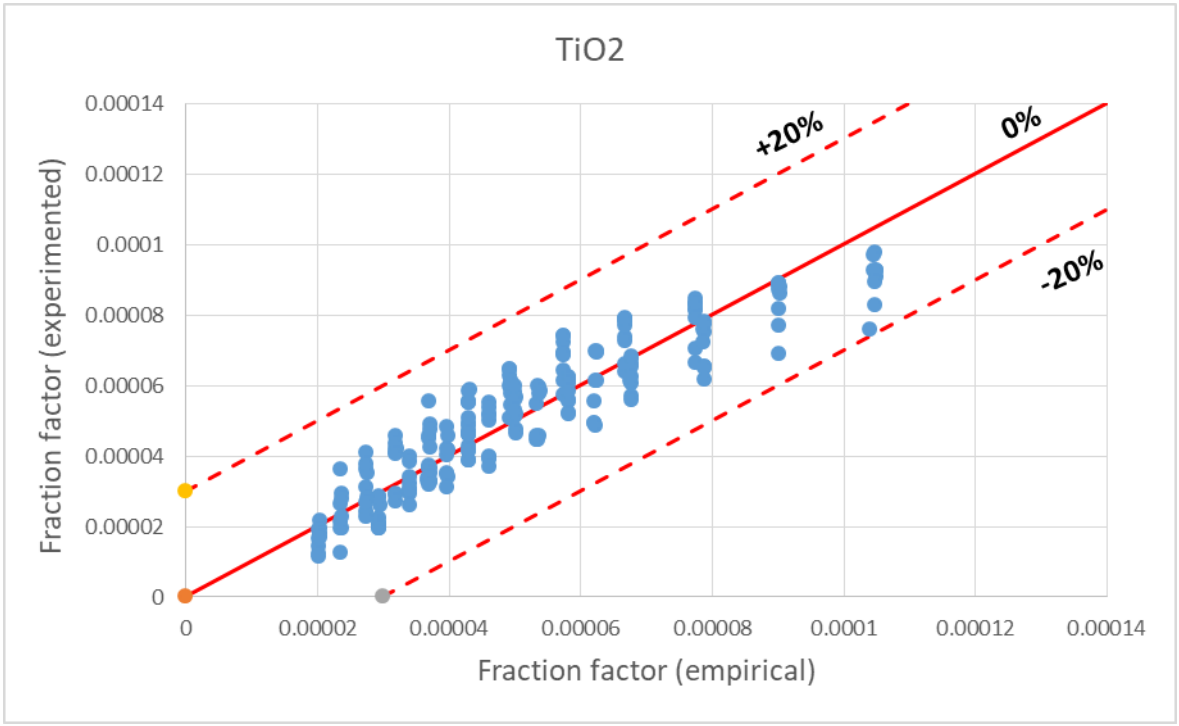

Figure 16 Relationship between Experimental and empirical results for Friction factor of TiO_2 nanofluid

CONCLUSIONS

For this research, a helical coil heat exchanger was designed and fabricated in the laboratory. Tests were conducted, and data was collected. Nanoparticles, according to the findings, considerably increase the heat transfer coefficient within the helical coil tube. Because of the turbulent flow effect, the Nusselt number increases as the Reynolds number within the tube increases. The nanofluid has also enhanced the Nusselt number. The Nusselt number climbs substantially as the volume concentration of nanoparticles TiO2 increases until it reaches its maximum value of 0.30%. The Nusselt number rises as a result of a drop in thermal conductivity, a rise in specific heat at constant pressure, and a temperature drop. Furthermore, increasing the volume concentration beyond the optimum amount has a slight impact on the Nusselt number because the nanoparticles gather and form a fouling layer that prevents heat transfer.

REFERENCES

[1]. Maghrabie, H.M., Attalla, M., Mohsen, A.A., 2021. Performance Assessment of a Shell and Helically Coiled Tube Heat Exchanger with Variable Orientations Utilizing Different Nanofluids. Appl. Therm. Eng. 182, 116013.

[2]. Huminic, G., Huminic, A.,2016. Heat Transfer and Flow Characteristics of Conventional Fluids and Nanofluids in Curved Tubes: A Review. Renew. Sustain. Energy Rev. 58, 1327–1347.

[3]. Prabhanjan, D.G., Raghavan, G.S.V., Rennie, T.J.,2002. Comparison of Heat Transfer rates between a straight Tube Heat Exchanger and a Helically Coiled Heat Exchanger. Int. Commun. Heat Mass Transf. 29, 185–191.

[4]. Alimoradi, A., Veysi, F., 2016. Prediction of Heat Transfer Coefficients of Shell and Coiled Tube Heat Exchangers using numerical method and experimental validation. Int. J. Therm. Sci. 107, 196–208.

[5]. Dravid, A.N., Smith, K.A., Merrill, E.W., Brian, P.L.T., 1971. Effect of secondary fluid motion on laminar flow Heat Transfer in Helically Coiled Tubes. Aiche J. 17,1114–1122.

[6]. Kumar, P.C.M., Chandrasekar, M., 2020. A Review on Helically Coiled Tube Heat Exchanger using Nanofluids. Mater. Today, Proc. 21, 137–141.

[7]. Fsadni, A.M., Whitty, J.P.M., Adeniyi, A.A., Simo, J., Brooks, H.L., 2018. A Review on the application of nanofluids in Coiled Tube Heat Exchangers. In Micro and Nanomanufacturing Springer 2, 443–465.

[8]. Kahani, M., Heris, S.Z., Mousavi, S. M., 2013. Comparative study between Metal Oxide Nanopowders on Thermal Characteristics of Nanofluid Flow through Helical Coils. Powder Technol. 246, 82–92.

[9]. Tohidi, A., Ghaffari, H., Nasibi, H., Mujumdar, A.S., 2015. Heat Transfer Enhancement by Combination of Chaotic Advection and Nanofluids Flow in Helically Coiled Tube. Appl. Therm. Eng. 86, 91–105.

[10]. Eiamsa-Ard, S., Wongcharee, K., 2018. Experimental Study of TiO_2-Water Nanofluid Flow in Corrugated Tubes Mounted with Semi-Circular Wing Tapes. Heat Transf. Eng., 39, 1–14.

[11]. Maddah, H., Aghayari, R., Farokhi, M., Jahanizadeh, S., Ashtary, K.,2014. Effect of Twisted-Tape Turbulators and Nanofluid on Heat Transfer in a Double Pipe Heat Exchanger. J. Eng.

[12]. Srinivas, T., Vinod, A.V., 2016. Heat Transfer Intensification in a Shell and Helical Coil Heat Exchanger using Water-Based Nanofluids. Chem. Eng. Process. Process Intensif., 102, 1–8.

[13]. Farajollahi, B., Etemad, S. G., Hojjat, M.,2010, Heat Transfer of Nanofluids in a Shell and Tube Heat Exchanger. Int. J. Heat Mass Transf., 53, 12–17.

[14]. Maxwell, J.C., 1904. A treatise on electricity and magnetism. Oxford University Press, Cambridge. Second ed.

[15]. Niwalkar, A.F., Kshirsagar, J.M., Kulkarni, K.,2019. Experimental Investigation of Heat Transfer Enhancement in Shell and Helically Coiled Tube Heat Exchanger using SiO_2/Water Nanofluids. Mater. Today, Proc. 18, 947–962.

[16]. Shahrul, I.M., Mahbubul, I.M., Saidur, R., Sabri, M.F.M., 2016. Experimental Investigation on Al_2O_3–W, SiO_2–W, And Zno–W Nanofluids and Their Application in a Shell and Tube Heat Exchanger. Int. J. Heat Mass Transf. 97, 547–558.

[17].Suresh, S., Chandrasekar, M., Sekhar, S.C., 2011. Experimental Studies on Heat Transfer and Friction Factor Characteristics of Cuo/Water Nanofluid Under Turbulent Flow in a Helically Dimpled Tube. Exp. Therm. Fluid Sci. 35, 542–549.
[18].Naik, B.A.K., Vinod, A.V.,2018. Heat Transfer Enhancement using Non-Newtonian Nanofluids in a Shell and Helical Coil Heat Exchanger. Exp. Therm. Fluid Sci. 90, 132–142.
[19].Ardekani, A.M., Kalantar, V., Heyhat, M.M., 2019. Experimental Study on Heat Transfer Enhancement of Nanofluid Flow Through Helical Tubes. Adv. Powder Technol. 30, 1815–1822.
[20].Singh, K., Sharma, S.K., Gupta, S.M., 2021. An Experimental Investigation of Hydrodynamic and Heat Transfer Characteristics of Surfactant-Water Solution and CNT Nanofluid in a Helical Coil-Based Heat Exchanger. Mater. Today, Proc., 43, 3896–3903.
[21].Kumar, P.C.M., Kumar, J., Suresh, S., 2013. Experimental Investigation on Convective Heat Transfer and Friction Factor in a Helically Coiled Tube with Al_2O_3/Water Nanofluid. J. Mech. Sci. Technol. 27, 239–245.